Digital Soil Mapping of Soil Organic Carbon Stock in Bhutan

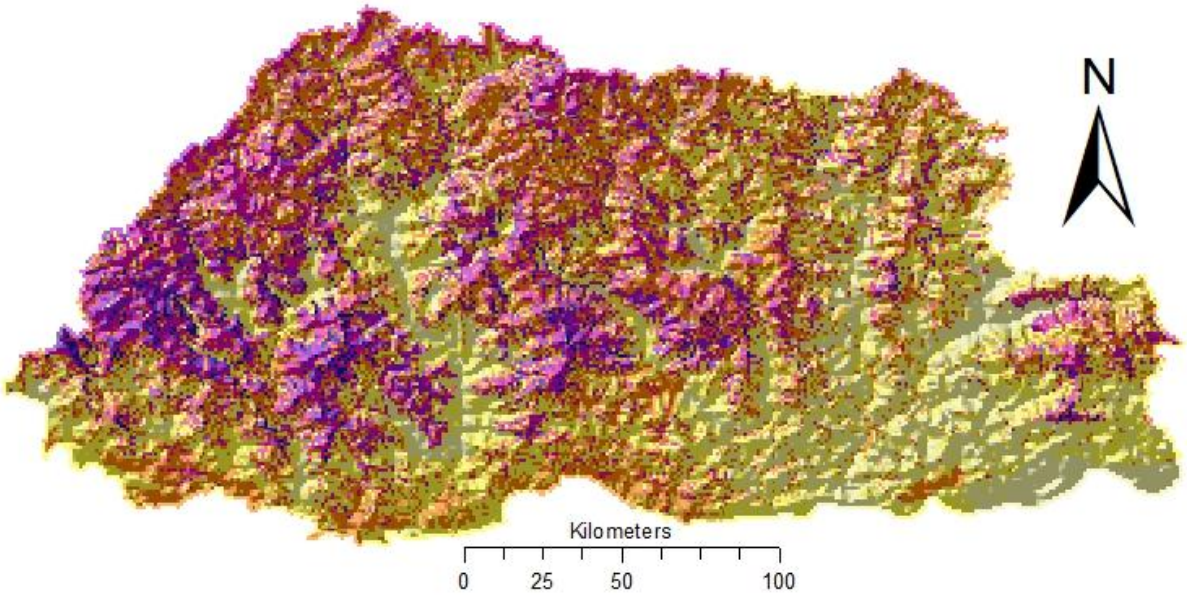

December 2017

National Soil Services Centre
Department of Agriculture
Ministry of Agriculture & Forests
Thimphu

Citation

NSSC (2017). Digital Soil Mapping of Soil Organic Carbon Stock in Bhutan. National Soil Services Centre. Department of Agriculture, Ministry of Agriculture and Forests, Royal Government of Bhutan, Thimphu.

Working Group Members

Tsheten Dorji, Senior Soil Survey & Land Evaluation Officer, NSSC
Sangita Pradhan, GIS Technician, NSSC
Dawa Tashi, Soil Survey & Land Evaluation Officer, NSSC
Dr. Karma Dema Dorji, Soil Specialist/Program Director, NSSC
Dr. Tshering Dorji, Principal Land Management Officer, NSSC

Table of Contents

Figures

Tables

1. Executive Summary

Soil organic carbon (SOC) plays an integral part in improving soil security, water security, food security, energy security, climate change abatement, biodiversity protection, and ecosystem services. This is largely because it has a significant influence on other soil physical, chemical, and biological properties. As such, it is often considered as a common indicator for soil security, water security, and ecosystem service delivery among others. Among the terrestrial carbon (C) pools, SOC is the largest constituting almost two-third of the global terrestrial C pool. Thus, SOC can either be a major C source or C sink depending upon the C fluxes which is primarily influenced by anthropogenic activities. This means that SOC plays a key role in the global C cycle and as such, would have a huge impact on climate change and delivery of various ecosystem services.

Since SOC varies in space and time, a clear knowledge about its quantity and spatial distribution would be vital to better understand the C dynamics. However, to date, not many countries have mapped their national SOC stock particularly in the developing countries. In this regard, Bhutan is no exception and there is paucity of information on SOC in the country. Because of limited knowledge on the quantity and spatial distribution of SOC in the country, Bhutan has not been able to clearly formulate plans and programs to increase C sequestration and enhance SOC storage. In order to facilitate such plans and programs for increasing resilience to climate change and enhancing ecosystem services, a preliminary mapping of SOC stock of Bhutan was carried out using digital soil mapping (DSM) techniques. The mapping was done with the specific objective to establish preliminary baseline information on SOC stock to facilitate proper research and management of SOC stock in the future.

SOC was digitally mapped using regression kriging (RK). A total of 993 soil data points was used for mapping SOC stock in the top 30 cm depth. Regression tree model (RTM) and ordinary kriging were used to perform the RK with elevation (DEM), land use land cover (LULC), slope, aspect, profile and plan curvatures, normalized difference vegetation index (NDVI), SAGA wetness index (SWI), mean precipitation, mean temperature, geology, and terrain ruggedness index (TRI) as environmental covariates. The model validation was done by repeated data splitting method. SOC density for each 1×1 km^2 grid cell was computed using the RK predicted SOC concentration and bulk density values.

The preliminary results show that for the top 30 cm depth, Bhutan stores about 0.4 GtC with SOC density ranging from 0.5 to 315.3 ton ha^{-1}. Among other environmental covariates, LULC, topography, and climatic factors had significant influence on the spatial distribution of SOC stock. The SOC stock was relatively low in the southern and eastern regions as opposed to the western and northern parts of the country. This is largely attributed to less forest cover and high rate of mineralization in the eastern and southern regions, respectively. Under different LULC types, the SOC stock was lowest under agriculture land and highest under forest, and this is in accordance with the results from other studies.

Similarly, the SOC stock for the upper one meter depth was estimated to be about 0.9 GtC. If we compare with the global SOC storage of 1500 GtC for the upper one meter, Bhutan stores about 0.1% of the global SOC stock despite its total land area accounting only about 0.02% of the global land area. This suggests that Bhutan stores almost five times more SOC stock than its total land area. This could be largely attributed to its large forest cover and good environment condition. However, to remain as a

C neutral/negative country, increasing SOC stock through enhanced C sequestration and protection of current SOC stock would be of paramount importance to Bhutan in the near future.

2. Introduction

Soil is essentially made up of minerals, organic matter/carbon, water, and air. Among these four main components, soil organic carbon (SOC) forms the integral part of a functional soil. This is largely because SOC has the ability to improve the soil physical, chemical, and biological properties, which can enhance soil security. Enhanced soil security can improve food security, water security, energy security, climate stability, biodiversity, and ecosystem services (McBratney *et al.*, 2014). SOC also plays a key role in global carbon (C) cycle as it is the largest terrestrial C pool. Because of the important role it plays, SOC is often considered as a common indicator for soil security, water security, and ecosystem services. Further, SOC stock is one of the three indicators in assessing Land Degradation Neutrality (LDN) status by 2030. Bhutan is an LDN country and information on its SOC stock and spatial distribution will be indispensable to assess LDN status by 2030.

Globally, soil stores about 1500 GtC (1 GtC = 10^{15}gC) in the top one meter (Jobbágy and Jackson, 2000) which is approximately three times as much C found in the biosphere and twice as much C found in the atmosphere. Assuming that other components of global C cycle remain constant, a change in global SOC storage by 1% may trigger a shift of about 8 ppm of CO_2 concentration in the atmosphere. This highlights the significance of C sequestration and storage in the soil to mitigate climate change. In order to increase C sequestration and storage, adequate information on the spatial distribution and storage of SOC is necessary to formulate appropriate land management and C sequestration strategies both at national and global scales. However, such information is limited in most of the countries, particularly in developing countries. This has posed a challenge to produce a global SOC stock map to facilitate proper SOC management for enhancing soil quality, reduce climate change, and enhance ecosystem services.

To this end, the Global Soil Partnership (GSP) initiated SOC stock mapping in all the member countries to produce the global SOC stock map. This initiative came as a blessing in disguise for Bhutan as it does not have a national SOC stock map. Further, SOC stock mapping is critical for Bhutan as it has been declared as a carbon neutral country in the world and requires such information in order to keep track of its national C status. In this regard, a first ever systematic SOC stock mapping for Bhutan was done to take stock of its SOC stock for the top 30 cm depth.

3. Aims & Objectives

The DSM of SOC stock in Bhutan was undertaken with the following objectives:

- Establish a national baseline information on SOC stock;
- Contribute to global SOC stock mapping initiated by the GSP;
- Contribute to better management of SOC through proper storage and enhanced C sequestration; and
- Build the national capacity on DSM.

4. Materials & Method

4.1 Study area

Bhutan is a landlocked country located in the Himalayas with China in the north and India in the east, west, and south. It has a geographical area of 38,394 square kilometres with rugged terrain characterized by 'V' shaped valleys and high peak mountains. The valleys are characterized by narrow alluvial floors, fans, and terraces, with the lower slopes and alluvia often mantled with colluvia from upslope and aeolian deposits (Baillie *et al.*, 2004; Caspari *et al.*, 2006; Dorji *et al.*, 2009). Within less than 200 km, the altitudinal gradient ranges from about 97 m to about 7570 m above mean sea level. As such, there are several agro-ecological zones with distinct climatic regimes in between. It has a monsoon type of climate with annual precipitation varying from more than 2000 mm in the south to less than 1000 mm in the north and central regions. The mean annual temperature ranges from approximately 14 to 26° C during summer to about -3 and 15° C in winter.

The mountains are young and still rising, leading to landscape dissection and natural soil erosion (Singh *et al.*, 2010); the latter process is continually affecting soil development. There are four main soil zones grouped based on altitude i.e. i) moderately weathered and leached thin dark topsoil over bright subsoil up to about 3000 m asl; ii) very bright orange-coloured non-volcanic andosolic soils and iii) acidic soils with thick surface litter that grade to weak podzols up to about 4000 m asl; and iv) alpine turf with deep dark and friable topsoil over yellowish subsoil mixed with raw glacial deposits above 4000 m asl (Baillie *et al.*, 2004).

More than 58% of Bhutan's population depends on agriculture, livestock and forestry for their livelihood. However, the cultivated agricultural land accounts only for about 3% of the total land area (LCMP, 2010) due to rugged terrain and extreme climatic conditions. As such, more than 70% of the total agriculture land is located on steep slopes with high incidence of soil erosion. On the other hand, about 71% of the country is under forest cover (LCMP, 2010) with very rich biodiversity. The spatial distribution of different LULC types is greatly influenced by altitude, slope, and climatic regime. Hence, broadleaf forest is predominant below 2500m asl and coniferous forest between 2500m and 3500m asl. However, shrub land and grassland occur all along the altitudinal gradient. As expected, snow and screes are confined to areas above 3500m asl. On the other hand, agriculture land is mostly located on valley bottoms and mountain foot slopes.

4.2 Soil Data Extraction

Soil information is limited in Bhutan as not many soil surveys have been done in the past. As such, its soil resources are basically unexplored and not fully known. However, a few detailed soil surveys was done in the past based on the client's request. Although these survey sites are not homogeneously distributed, they do represent the major parts of the country. For mapping the SOC stock of Bhutan, a total of 993 data points, from previous soil surveys (1997- to date), was extracted from the Bhutan Soil Database (BHUSOD) maintained by the National Soil Services Centre under the Department of Agriculture (Fig. 4.1). More than 80% of the total soil data was from soil profile pits while the remaining was from auger bore holes. A standard soil survey method was followed to collect the soil

data. Soils were described and sampled based on genetic horizons. Soil samples were analyzed for various soil parameters including carbon (C) concentration using Walkley and Black (1934) and bulk density using core ring method (Blake *et al.*, 1986).

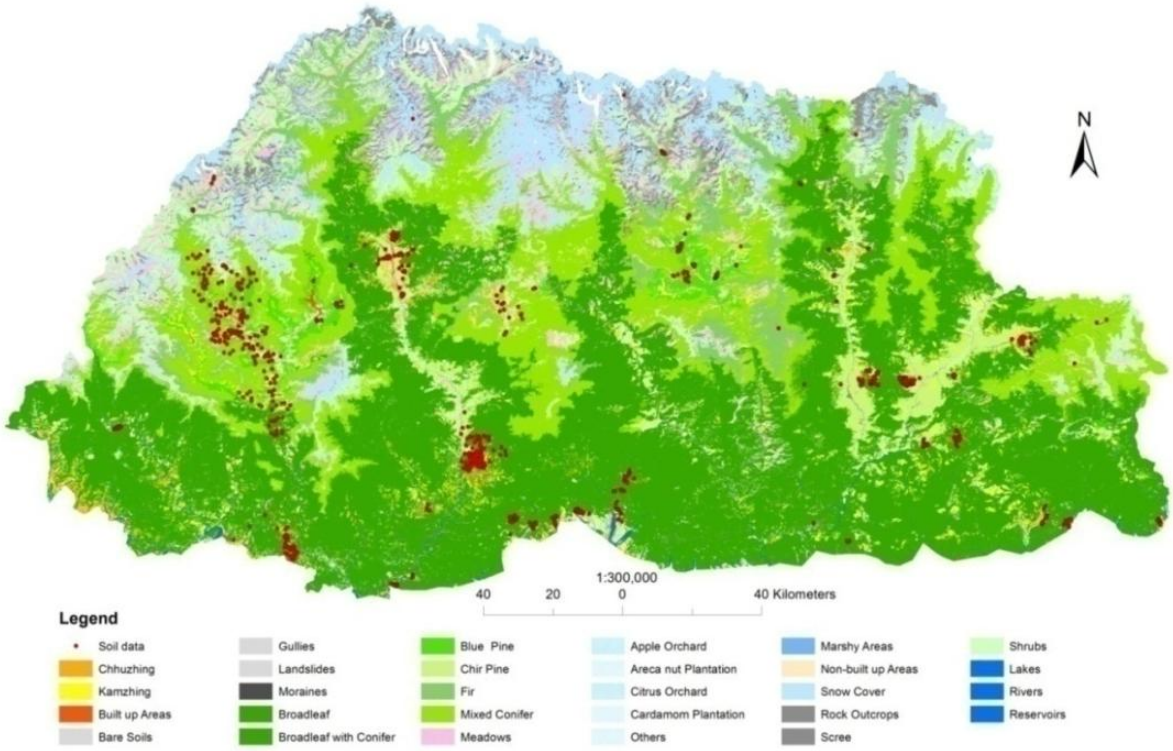

Figure 4.1 Distribution of soil observation sites

Since soil samples were collected based on genetic horizons, they were from different soil depths. This posed a challenge to digitally map SOC stock for a particular depth. In this regard, an equal-area spline function was fitted to the profile values of the target soil variables using the CSIRO Spline Tool V2 (ASRIS, 2011) to convert the horizon-based values to the desired soil depth (0-30 cm). The equal-area spline function is based on the quadratic spline model of Bishop *et al.* (1999). It assumes that the true soil attribute values vary smoothly with depth, which can be translated into mathematical terms by denoting depth by x, and the depth function describing the true attribute values by $f(x)$ such that, $f(x)$ and its first derivative (x) are both continuous, and that $f^{'}(x)$ is square integrable. The depths of the boundaries of the n layers are given by $x0 < x1 ; \ldots < xn$. The measurement of the bulk sample from horizon i is assumed to reflect the mean attribute level, apart from measurement error. The measurements $y_i(i = 1, \ldots n)$ are therefore mathematically modeled as

$$y_i = f_i + e_i \qquad (1)$$

where $\overline{f}_{\mathrm{i}} = \int_{x_{i-1}}^{x_i} f(x)dx/(x_i\ x_{i-1})$ is the mean value of $f(x)$ over the interval (x_{i-1}, x_i). The errors e_i are assumed independent, with mean 0 and common variance σ^2. $f(x)$ represents a spline function, which can be determined by minimizing:

$$\frac{1}{n}\sum_{i=1}^{n}(y_i - \bar{f}_i)^2 + \lambda\int_{x_0}^{x_n}[f^m(x)]^2\,dx \quad (2)$$

The first term depicts the fit to data while the second term measures the roughness of function $f(x)$, expressed by its first derivative $f(x)$. Parameter λ controls the trade-off between the fit and the roughness penalty. The solution is linear-quadratic smoothing spline, linear between layers, and quadratic within layers (Bishop *et al.*, 1999; Malone *et al.*, 2009).

4.3 Acquisition and Derivation of environmental covariates

Digital Soil Mapping (DSM) of any soil property hinges on the use of easily discernable ancillary soil and/or environmental attributes. To generate the terrain attributes, a 30m DEM covering whole Bhutan was extracted from the Shuttle Radar Topography Mission (SRTM) elevation data portal (http://earthexplorer.usgs.gov) and was re-sampled to 1 km resolution. Slope gradient, aspect, slope curvatures (profile and plan), SAGA wetness index (SWI), and terrain ruggedness index (TRI) were derived from the DEM using the System for Automated Geo-scientific Analysis (SAGA) software (http://www.saga-gis.org/en/index.html) and Arc GIS software (version 10.3).

Based on Moore *et al.* (1993), who characterized terrain-determined spatial variations in soil moisture content by a terrain index, the SWI was computed as tangent function of slope angle β and modified specific catchment area (SCA_M) (Böhner and Selige, 2006) (Eq. 3). The SCA_M is a function of slope angle β and the neighbouring maximum values SCA_{max} (Eq. 4).

$$SWI = \ln(SCA_M/\tan\beta) \quad (3)$$

$$SCA_M = SCA_{max}\,(1/15)^{\beta \exp(15^{\beta})} \quad for \quad SCA < SCA_{max}\,(1/15)^{\beta \exp(15^{\beta})} \quad (4)$$

where SCA is the specific catchment area defined as the corresponding drainage area per unit contour width (m^2m^{-1})(Böhner and Selige, 2006). The TRI indicates elevation difference between adjacent cells of a digital elevation grid. The process basically calculates the difference in elevation values from a centre cell and the eight cells immediately surrounding it. It squares each of the eight elevation difference values to make them all positive and averages the squares. The TRI is then derived by taking the square root of this average, and corresponds to average elevation change between any point on a grid and its surrounding area (Riley *et al.*, 1999).

$$TRI = Y\left[\sum(x_{ij} - x_{00})^2\right]^{1/2} \quad (5)$$

where x_{ij} = elevation of each neighbor cell to cell (0,0). In addition to the above covariates, the LULC data (LCMP, 2010), geological map (Department of Geology and Mines), mean temperature and precipitation (www.worldclim.org), and normalized difference vegetation index ($NDVI$) were used as covariates after re-sampling them to 1 km resolution. $NDVI$ is the sum of the reflectivity of near infrared (NIR) light subtracted from the reflectivity of the red light divided by the sum of the reflectivity of NIR light plus the reflectivity of the red light (Eq. 6).

$$NDVI = \frac{(NIR-Red)}{(NIR+Red)} \quad (6)$$

Based on the health of vegetation, there is a differential absorption and reflection of visible (0.4 to 0.7 µm) and NIR light (0.7 to 1.1 µm) of the electromagnetic spectrum. The $NDVI$ uses the visible and NIR regions to represent the health of the vegetation. Apart from this, $NDVI$ could be used to assess crop yield, photosynthetic activity of plants, and drought.

$NDVI$ was calculated using 3 datasets of Landsat-8 (Table 2.1) with free cloud cover (https://earthexplorer.usgs.gov/).

Table 2.1 Landsat-8 datasets used in the study

Sl #	Scene ID	Row/Path	Cloud cover (%)	Acquisition date
1	LC81370412016303LGN00	41/137	2.59	2016.10.09
2	LC81380412015323LGN00	41/138	7.96	2015.11.19
3	LC81390412015362LGN00	41/139	1.37	2015.12.28

Prior to calculating the $NDVI$, all data were converted to actual land surface reflectance products (Top of Atmosphere (TOA)) using the rescaling parameters that comes with a metadata file. The necessary correction was done using the following equation (Eq. 7):

$$\rho\lambda' = M_\rho Q_{cal} + A_\rho \quad (7)$$

where $\rho\lambda'$ is TOA planetary reflectance without correction for solar angle, M_ρ is band-specific multiplicative rescaling factor, Q_{cal} is quantized and calibrated standard product pixel values (DN), and A_ρ is band-specific additive rescaling factor.

Further, the surface reflectance products were corrected for sun angle using Eq. 8:

$$\rho\lambda' = \frac{\rho\lambda'}{\cos(\theta_{SZ})} = \frac{\rho\lambda'}{\sin(\theta_{SE})} \quad (8)$$

where $\rho\lambda'$ is TOA planetary reflectance, θ_{SZ} is local solar zenith angle ($\theta_{SZ} = 90° - \theta_{SE}$), and θ_{SE} is local sun elevation angle (degree).

4.4 Spatial modeling of SOC concentration and bulk density at 30cm depth

Digital Soil Mapping (DSM) of any soil property is done with the assumption that a soil property of interest is closely associated with easily discernible ancillary environmental variables. This enables the target variable to be predicted by establishing relationships between it and the ancillary variables (McBratney *et al.*, 2003). Based on this assumption, several methods have been used to digitally map the target variable. Odeh *et al.* (1995) compared several methods of DSM: multi-linear regression, ordinary kriging, universal kriging, isotopic co-kriging, heterotopic co-kriging, and some variants of regression kriging (RK) models, and found out that RK model to be most superior. A later study

reported RK model to be more practical and robust than other prediction models (Minasny and McBratney, 2007). As such, we used the RK model.

RK has two main components i.e. regression and kriging (Fig. 4.2). For the regression part, regression tree model (RTM) was used (Cubist 2.09 package) with elevation (DEM), LULC, slope, aspect, profile and plan curvatures, NDVI, SWI, mean precipitation, mean temperature, geology, and TRI as covariates to predict the target variable. The RTM is robust and appropriate for complex landscapes, such as in the Himalayas. The RTM is a non-parametric prediction model, which predicts the target variable based on linear regression models instead of discrete values predicted by the classical tree models (Minasny and McBratney, 2008).

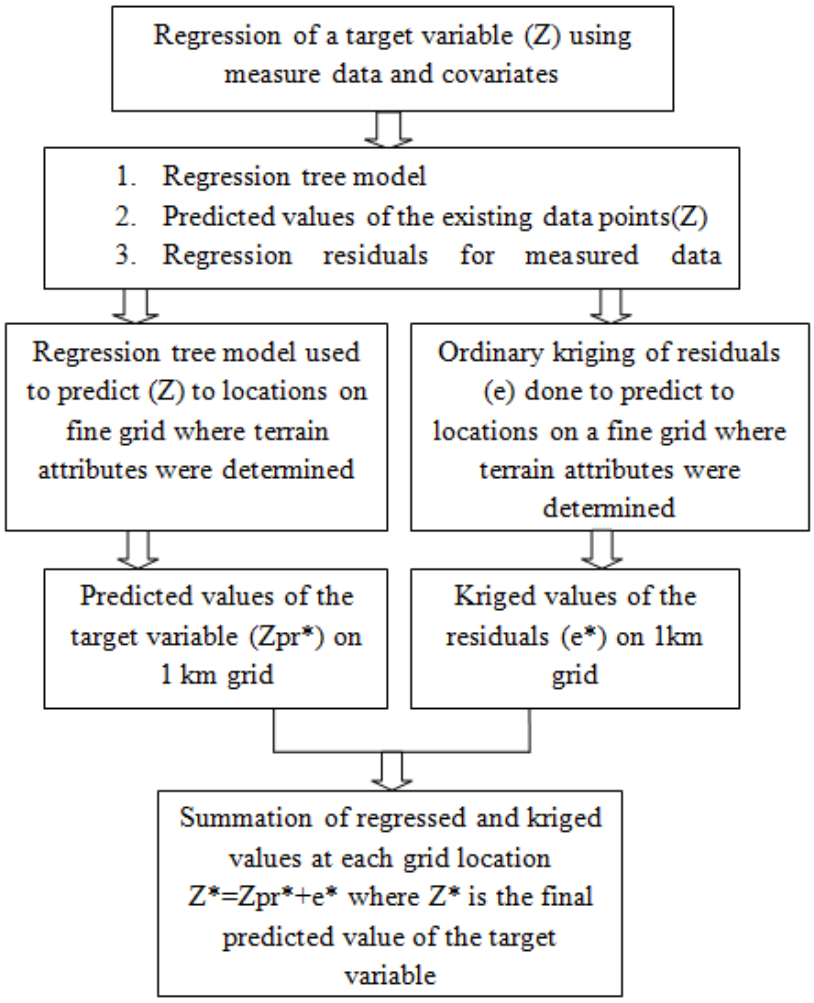

Figure 4.2 Flow chart showing the steps of RK for DSM (adapted from Odeh et al. (1995)).

At each node of the tree model, conventional linear least-squares regression is used to create the model associated with each of the terminal rules. Thus, the model generates a set of comprehensible rules, each of which has an associated multivariate linear model. When the rule conditions are met, the model predicts the target variable for each grid cell that has values for the appropriate predictor covariates (Minasny and McBratney, 2008). For the kriging part, the residuals, which are the difference between

the measured and regressed values, were interpolated onto the entire 1 km grid, using a simple kriging, embedded in the package: Variogram Estimation and Spatial Prediction plus Error (VESPER) (Minasny *et al.*, 2005). The final predicted value of the target variable at each 1 km grid cell was computed by summing up the regressed value from the RTM and the kriged residual (Fig. 4.2).

4.5 Data Validation

Any prediction model needs to be validated to assess its accuracy and reliability. It can be done either through external or internal validation. The former uses a new validation dataset from the same or similar population for validating previous models and is considered to be relatively better than internal validation methods. However, the difficulty in obtaining a new independent external dataset forces to go for internal validation. Repeated data splitting is a common internal validation method and we used this to validate our models. The whole data was partitioned into two portions, called the training and validation datasets. The training dataset constituted 70% of the total data points (698 points) and was selected through a simple random sampling procedure. The remaining data (30%) was used as a validation dataset. Firstly, RTM was fitted onto the training dataset (using Cubist 2.09) and the model was used to predict the target variable for the validation dataset. Secondly, the residuals for the training dataset were calculated by subtracting the regressed values from the measured values of the target variable. Thirdly, the residuals of the training dataset were kriged to predict the residuals of the validation dataset using VESPER. The final RK prediction for the validation dataset was obtained by summing the regressed values from RTM and kriged values (Fig. 4.2). In order to assess the performance of the RK model, the RK predicted values (regressed plus kriged values) were plotted against the measured values of the validation dataset. This whole process was repeated for 10 times to assess the stability of the prediction accuracy of the RK model. At each iteration, the statistical parameters including: (i) root mean square error (RMSE), (ii) coefficient of correlation (*R*), (iii) coefficient of determination (R^2), and (iv) mean error (ME) were determined and averaged at the end to provide the overall prediction accuracy of the model. The RMSE, which provides a measure of accuracy of the prediction method, is defined as:

$$\text{RMSE} = \sqrt{\frac{1}{n}\sum_{j=i}^{n}\left[z(s_j) - z^*(s_j)\right]^2} \quad (9)$$

and the ME (Odeh *et al.*, 1995), which measures bias of prediction, is defined as:

$$\text{ME} = \frac{1}{n}\sum\left[z(s_j) - z^*(s_j)\right] \quad (10)$$

where $z(s_j)$ and $z^*(s_j)$ are the observed and predicted values, respectively (Eqs. 9 and 10). For more accurate prediction the RMSE should be as small as possible while the ME should be close to zero.

4.6 Computing SOC stock

Although SOC density and SOC stock are often used interchangeably in literature (Minasny *et al.*, 2006), they differ in scale and unit. SOC density is the SOC mass per unit area for a given depth, which can be calculated as:

$$SOC_d\ (kg\ m^{-2}) = SOC\ (kg/kg) * BD\ (kg\ m^{-3}) * D(m) \quad (11)$$

where SOC_d is SOC density (kg m^{-2}), SOC is SOC concentration (kg/kg), BD is bulk density (kg m^{-3}) and D is depth interval thickness (m). On the other hand, SOC stock is the actual SOC mass for a given soil depth and area. It was calculated by summing up the product of SOC density and area of the smallest mapping unit e.g. grid cell 1 × 1km^2.

$$SOC_{st}(t) = \sum_{i=1}^{n}\{(SOC_{di} * A_i)/10^3\} \quad (12)$$

where SOC_{st} is SOC stock in metric tonne (t), n is number of 1 km grid cells, SOC_{di} is SOC density of grid cell for a particular depth interval (kg m^{-2}), A_i is an area of 1 km grid cell (1km^2) and 10^3 is the unit conversion factor.

5. Results

5.1 Spatial modelling of SOC concentration and bulk density

As shown in Table 5.1, the RTM, based on the whole dataset (993 data), used MT, GEO, NDVI, PLCUR, SLOPE, ASP, MP, and ALT as conditions to perform the regression for SOC concentration. However, MP, MT, ALT, NDVI, TRI, SLOPE, ASP, SWI, PLCUR, and PRCUR were used as environmental covariates to predict the SOC concentration. Similarly for bulk density, MP, ALT, SWI, MT, PRCUR, NDVI and ASP were used as conditions and MT, MP, ALT, NDVI, TRI, SWI, SLOPE, PRCUR, PLCUR, and ASP as environmental covariates. Among the environmental covariates, MP, MT, ALT, and NDVI showed more influence on both SOC concentration and bulk density, and their spatial distributions.

Table 5.1 Usage (%) of covariates in the RTM for predicting SOC and bulk density (0-30 cm depth).

	SOC Concentration (0-30 cm depth)			
Attribute usage				
Conditions (Usage in %)	MT (99%)	GEO (72%)	NDVI (43%)	PLCUR (32%)
	SLOPE (25%)	ASP (24%)	MP (13%)	ALT (9%)
Environmental covariates used in regression tree model (Usage in %)	MP (89%)	MT (86%)	ALT (70%)	NDVI (60%)
	TRI (57%)	SLOPE (48%)	ASP (46%)	SWI (41%)
	PLCUR (14%)	PRCUR (11%)		
	Bulk density			
Conditions (Usage in %)	MP (75%)	ALT (49%)	SWI (45%)	MT (32%)
	PRCUR (12%)	NDVI (9%)	ASP (8%)	
Environmental covariates used in regression tree model (Usage in %)	MT (99%)	MP (95%)	ALT (91%)	NDVI (81%)
	TRI (74%)	SWI (67%)	SLOPE (62%)	PRCUR (31%)
	PLCUR (20%)	ASP (13%)		

TRI terrain ruggedness index, *SWI* SAGA wetness index, *NDVI* normalized difference vegetation index, *MT* mean temperature, *MP* mean precipitation, *ASP* aspect, *PLCUR* plain curvature, *PRCUR* profile curvature, *ALT* altitude.

Overall, the RTM performed well as indicated by the low average error, and ME for both SOC concentration and bulk density (Table 5.2). The average error was 0.89 g/100 gm for SOC stock and

0.05 g cm^{-3} for bulk density. The relative errors of both SOC stock and bulk density were less than 1. The coefficient of determination (R^2) was 0.59 for SOC concentration and 0.88 for bulk density. The RMSE for SOC and bulk density was 1.34 and 0.09 g cm^{-3}, respectively. Looking at the ME, the RTM was less bias in predicting bulk density than SOC concentration as its values were much closer to zero.

Table 5.2 Performance of RTM in predicting SOC concentration and bulk density.

Depth (cm)	SOC (g/100gm)					Bulk density (g cm^{-3})				
	AE	RE	ME	RMSE	R^2	AE	RE	ME	RMSE	R^2
0 – 30	0.89	0.61	0.05	1.31	0.59	0.05	0.23	0.0002	0.09	0.92

SOC soil organic carbon, AE average error, RE relative error, ME mean error, RMSE root mean square error, R correlation coefficient, R^2 coefficient of determination

5.2 Validation of RTM and RK Models

Judging by the statistical parameters (Table 5.3), based on ten iterations, the overall RTM prediction for both SOC concentration and bulk density is good with mean R^2 of 0.63 and 0.93, respectively. However, when compared between SOC concentration and bulk density, the RTM did much better in predicting bulk density than SOC concentration. Table 5.4 depicts the overall performance of RK in predicting the SOC. Going by the statistical parameters, the RK did very well in predicting SOC compared to RTM with R^2 of 0.87, RMSE of 1.23, and ME of 0.02. This indicates that RK is better than RTM in DSM.

Table 5.3 Validation results of RTM in predicting SOC and bulk density (0-30 cm depth).

n	SOC (g/100g)					Bulk density (g cm^{-3})				
	AE	RE	ME	RMSE	R^2	AE	RE	ME	RMSE	R^2
V1	0.83	0.56	0.05	1.68	0.62	0.04	0.16	0.01	0.11	0.94
V2	0.74	0.53	0.22	1.67	0.67	0.04	0.17	-0.01	0.10	0.92
V3	0.83	0.60	-0.10	1.68	0.59	0.04	0.19	-0.01	0.10	0.92
V4	0.83	0.55	-0.01	1.61	0.69	0.04	0.17	0.01	0.12	0.92
V5	0.91	0.64	0.20	1.59	0.56	0.03	0.15	0.00	0.11	0.94
V6	0.82	0.54	-0.15	1.56	0.67	0.04	0.17	0.00	0.10	0.92
V7	0.78	0.55	0.10	1.68	0.64	0.04	0.18	0.00	0.10	0.90
V8	0.84	0.60	0.19	1.60	0.59	0.04	0.17	0.01	0.11	0.92
V9	0.77	0.53	0.00	1.74	0.67	0.04	0.16	0.00	0.38	0.94
V10	0.81	0.56	-0.04	1.54	0.64	0.04	0.16	0.00	0.10	0.94
Mean	0.82	0.57	0.05	1.63	0.63	0.04	0.17	0.01	0.13	0.93

SOC soil organic carbon, *AE* average error, *RE* relative error, *ME* mean error, *RMSE* root mean square error, *R* correlation coefficient, R^2 coefficient of determination, *n* number of iterations

Table 5.4 Performance of RK in predicting SOC concentration.

Depth (cm)	SOC (g/100gm)		
	ME	RMSE	R^2
0 – 30	0.02	1.23	0.87

SOC soil organic carbon, AE average error, RE relative error, ME mean error, RMSE root mean square error, R correlation coefficient, R^2 coefficient of determination

5.3 Spatial distribution of SOC stock

SOC density for each 1×1 km^2 grid was computed using the RK predicted SOC concentration and bulk density values. The spatial distribution of SOC density was greatly influenced by LULC, which is directly controlled by climate and topography of the area. Under different LULC types, the mean SOC density for the upper 30 cm depth decreased in the order of mixed conifer forest> fir forest> others> grassland> shrub land> blue pine forest> marshy land> horticulture> dry land> paddy land> built-up areas> chirpine forest (Table 5.5). Similarly, the effect of topography was also very clear with SOC density lowest on valley bottoms and lower mountains slopes as opposed to higher SOC density on the upper slopes. This is in line with the results reported by Dorji *et al.* (2014).

Table 5.5 Predicted SOC density under different LULC types (0-30 cm depth).

Sl #	LULC type	Mean SOC (ton/ha)	Sl#	LULC type	Mean SOC (ton/ha)
1	Paddy land	62.16	8	Fir Forest	102.35
2	Dry land	64.05	9	Mixed Conifer Forest	105.21
3	Built Up Areas	60.52	10	Grassland	98.26
4	Degraded Land	81.75	11	Horticulture	71.58
5	Broadleaf Forest	75.35	12	Marshy Area	74.1
6	Blue Pine Forest	84.79	13	Shrubland	92.49
7	Chir Pine Forest	51.54	14	Others	101.42

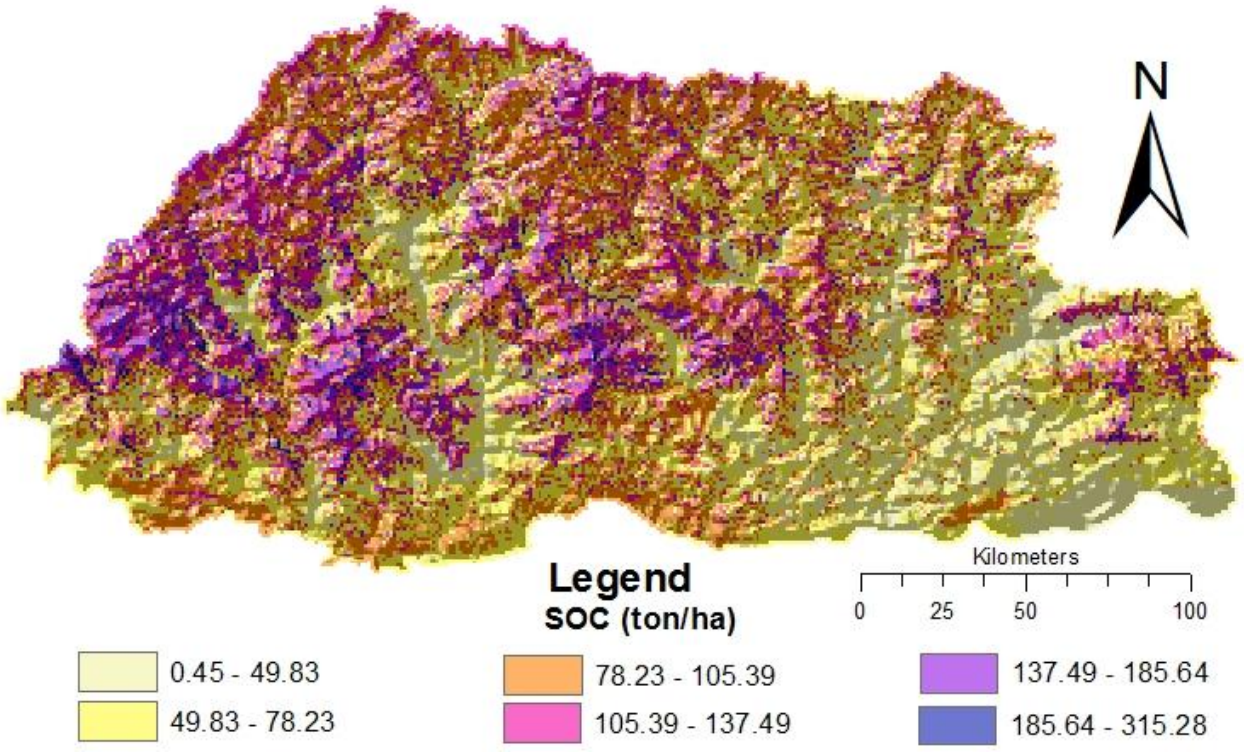

Figure 5.1 Predicted SOC density (1×1 km^2 grid) for the top 30 cm depth.

The SOC stock for each grid was computed (Eq. 12) and added to estimate the overall SOC stock for the entire country. The preliminary results show that for the top 30 cm depth, Bhutan stores about 0.4 GtC with SOC density ranging from 0.45 to 315.28 ton ha^{-1}. As expected, the spatial distribution of SOC stock was also similar to the spatial distribution of SOC density with LULC, topography, and climatic regime as the main influencing factors. The SOC stock in the southern and eastern regions was relatively small as opposed to the western and northern parts of the country (Fig. 5.1). This is chiefly due to less forest cover and high rate of mineralization in the eastern and southern regions, respectively. The SOC stock under different LULC types was quite similar to what Dorji *et al.* (2014) reported with SOC stock lowest under agriculture land and highest under forest.

Dorji *et al.* (2014) did digital soil mapping of SOC stock under different LULC types and reported high spatial variation of SOC stock under different LULC types. The study also reported that the SOC variation decreased with soil depth indicating that the influence of factors affecting SOC are maximum on the upper parts of the soil profile.

Table 5.6 Predicted SOC density under different LULC types (0-100 cm depth) (Dorji *et al.*, 2014).

LULC type	SOC (ton/ha)	LULC type	SOC (ton/ha)
Fir Forest	414.4	Blue Pine Forest	182.1
Mixed Conifer Forest	335.8	Dry Land	173.2
Shrubland	302.5	Orchard	133.4
Grassland	286.3	Paddy Land	120.1
Broadleaf Forest	263.5		

If we extrapolate these findings to rest of the country, Bhutan would roughly store about 0.9 GtC in the top one meter depth. The global SOC storage for the top one meter depth is about 1500 GtC (Jobbágy and Jackson, 2000) and, if so, then Bhutan stores about 0.1% of the global SOC stock despite constituting only about 0.02% of the global land area. This suggests that Bhutan stores almost five times more SOC stock than its total land area. This could be largely because of its large forest cover (71%) and good environment condition. Therefore, the large SOC stock in Bhutan needs to be protected and better managed through sustainable management of land and land-based natural resources to reduce climate change and provide continuous ecosystem services in the country and beyond. And further, to maintain its C neutral/negative status in the world.

6. Recommendations

This is the first attempt made to digitally map SOC stock in Bhutan for the top 30 cm depth. While doing so, many challenges were encountered at various levels. In order to overcome these challenges, the following recommendations are made:

- Need to generate more soil information covering the whole country;
- The NSSC staff needs to be trained on digital soil mapping (DSM) and statistical analysis;
- Statistical software needs to be procured for DSM;
- Should have easy access to existing data that are required for DSM;

- Need to collaborate with relevant agencies, both within and outside the country, for DSM; and
- Provide adequate financial support for DSM.

7. Conclusions

The preliminary results show that Bhutan stores about 0.4 and 0.9 GtC in the top 30 cm and 100 cm depths, respectively. When this is compared to the global SOC storage, Bhutan stores more than 0.1% of the global SOC stock which is almost five times more than its total land area. However, the next challenge for Bhutan would be to remain as a major global SOC storage and sink to stay as a C neutral/negative country. This could be done through sustainable management of soil and watershed to increase C sequestration, reduce C emission, and enhance C storage in the soil.

The SOC stock reported here has been estimated based on a small soil dataset. As such, the model predicted SOC stock may not be so accurate and might have a high degree of uncertainty. In this regard, the result presented here should be used cautiously. However, a more comprehensive SOC stock map of Bhutan will be produced once the National Forestry Inventory C data ($4\times4km^2$) becomes available.

References

ASRIS, 2011. ASRIS - Australian Soil Resource Information System. http://.asris.csrio.au. Accessed November 7, 2012.

Baillie, I.C., Tshering, K., Dorji, T., Tamang, H.B., Dorji, T., Norbu, C., Hutcheon, A.A., Bäumler, R., 2004. Regolith and soils in Bhutan, Eastern Himalayas. European Journal of Soil Science 55, 9-27.

Bishop, T.F.A., McBratney, A.B., Laslett, G.M., 1999. Modelling soil attribute depth functions with equal-area quadratic smoothing splines. Geoderma 91, 27-45.

Blake, G.R., Hartge, K.H., Klute, A., 1986. Bulk density. Methods of soil analysis. Part 1. Physical and mineralogical methods. SSSA Book Series, 363-375.

Böhner, J., Selige, T., 2006. Spatial prediction of soil attributes using terrain analysis and climate regionalisation. Böhner, J., McCloy, K.R., Strobl, J. (Eds.), SAGA-Analyses and Modelling Applications. Göttinger Geographische Abhandlungen. Vol. 115, pp. 13-28.

Caspari, T., Bäumler, R., Norbu, C., Tshering, K., Baillie, I., 2006. Geochemical investigation of soils developed in different lithologies in Bhutan, Eastern Himalayas. Geoderma 136, 436-458.

Dorji, T., Caspari, T., Bäumler, R., Veldkamp, A., Jongmans, A., Tshering, K., Dorji, T., Baillie, I., 2009. Soil development on Late Quaternary river terraces in a high montane valley in Bhutan, Eastern Himalayas. Catena 78, 48-59.

Dorji, T., Odeh, I.O.A., Field, D.J., Baillie, I.C., 2014. Digital soil mapping of soil organic carbon stocks under different land use and land cover types in montane ecosystems, Eastern Himalayas. Forest Ecology and Management 318, 91-102.

Jobbágy, E.G., Jackson, R.B., 2000. The vertical distribution of soil organic carbon and its relation to climate and vegetation. Ecological Applications 10, 423-436.

LCMP, 2010. Land cover mapping project. Technical Report. Ministry of Agriculture and Forests, Royal Government of Bhutan, Thimphu. http://www.nssc.gov.bt/bhutan-land-cover-assessment-2010 (accessed on 29 September 2012).

Malone, B.P., McBratney, A.B., Minasny, B., Laslett, G.M., 2009. Mapping continuous depth functions of soil carbon storage and available water capacity. Geoderma 154, 138-152.

McBratney, A., Field, D.J., Koch, A., 2014. The dimensions of soil security. Geoderma 213, 203-213.

McBratney, A.B., Mendonça Santos, M.L., Minasny, B., 2003. On digital soil mapping. Geoderma 117, 3-52.

Minasny, B., McBratney, A.B., 2007. Spatial prediction of soil properties using EBLUP with the Matérn covariance function. Geoderma 140, 324-336.

Minasny, B., McBratney, A.B., 2008. Regression rules as a tool for predicting soil properties from infrared reflectance spectroscopy. Chemometrics and Intelligent Laboratory Systems 94, 72-79.

Minasny, B., McBratney, A.B., Mendonça-Santos, M.L., Odeh, I.O.A., Guyon, B., 2006. Prediction and digital mapping of soil carbon storage in the Lower Namoi Valley. Soil Research 44, 233-244.

Minasny, B., McBratney, A.B., Whelan, B.M., 2005. VESPER version 1.62. Australian Centre for Precision Agriculture, McMillan Building A05, The University of Sydney, NSW 2006. http://www.usyd.edu.au/su/agric/acpa (accessed on 1st July 2012).

Moore, I.D., Gessler, P.E., Nielsen, G.A., Peterson, G.A., 1993. Soil attribute prediction using terrain analysis. Soil Science Society of America Journal 57, 443-452.

Odeh, I.O.A., McBratney, A.B., Chittleborough, D.J., 1995. Further results on prediction of soil properties from terrain attributes: heterotopic cokriging and regression-kriging. Geoderma 67, 215-226.

Riley, S.J., DeGloria, S.D., Elliot, R., 1999. A terrain ruggedness index that quantifies topographic heterogeneity. Intermountain Journal of Soil Science 5.

Singh, S.P., Singh, V., Skutsch, M., 2010. Rapid warming in the Himalayas: ecosystem responses and development options. Climate and Development 2, 221(212).

Walkley, A., Black, I.A., 1934. An examination of the Degtjareff method for determining soil organic matter, and a proposed modification of the chromic acid titration method. Soil Science 37, 29-38.